Featured in Physics

Agnostic Phase Estimation

Xingrui Song,[1] Flavio Salvati,[2] Chandrashekhar Gaikwad,[1] Nicole Yunger Halpern,[3,4]
David R. M. Arvidsson-Shukur,[5] and Kater Murch[1]

[1]*Department of Physics, Washington University, St. Louis, Missouri 63130, USA*
[2]*Cavendish Laboratory, Department of Physics, University of Cambridge, Cambridge, CB3 0HE, United Kingdom*
[3]*Joint Center for Quantum Information and Computer Science, NIST and University of Maryland, College Park, Maryland 20742, USA*
[4]*Institute for Physical Science and Technology, University of Maryland, College Park, Maryland 20742, USA*
[5]*Hitachi Cambridge Laboratory, J. J. Thomson Avenue, Cambridge CB3 0HE, United Kingdom*

The goal of quantum metrology is to improve measurements' sensitivities by harnessing quantum resources. Metrologists often aim to maximize the quantum Fisher information, which bounds the measurement setup's sensitivity. In studies of fundamental limits on metrology, a paradigmatic setup features a qubit (spin-half system) subject to an unknown rotation. One obtains the maximal quantum Fisher information about the rotation if the spin begins in a state that maximizes the variance of the rotation-inducing operator. If the rotation axis is unknown, however, no optimal single-qubit sensor can be prepared. Inspired by simulations of closed timelike curves, we circumvent this limitation. We obtain the maximum quantum Fisher information about a rotation angle, regardless of the unknown rotation axis. To achieve this result, we initially entangle the probe qubit with an ancilla qubit. Then, we measure the pair in an entangled basis, obtaining more information about the rotation angle than any single-qubit sensor can achieve. We demonstrate this metrological advantage using a two-qubit superconducting quantum processor. Our measurement approach achieves a quantum advantage, outperforming every entanglement-free strategy.

Phase estimation is crucial to quantum information processing: In several algorithms, phase estimation identifies unitary operators' eigenvalues [1–6]. Furthermore, phase estimation serves in quantum metrology, the use of quantum systems to probe and estimate physical parameters [7–9]. Conventionally, phase estimation requires prior knowledge about the unitary being probed.

For example, consider a unitary e^{iH} generated by a Hamiltonian H. In quantum algorithms, phase estimation encodes in a qubit register an estimate of an e^{iH} eigenvalue [10,11]. To perform this encoding, one initializes another register in an H eigenstate. Without information about H, conventional algorithmic phase estimation fails.

In quantum metrology, phase estimation is used to infer some unknown parameter α in a unitary $U_\alpha = e^{i\alpha A}$. The Hermitian generator $A = \sum_i a_i |a_i\rangle\langle a_i|$ has eigenstates $|a_i\rangle$ and eigenvalues a_i. α could quantify an unknown field's strength. One can estimate α by applying U_α to several quantum systems and measuring them. The optimal single-qubit probe states are the equal-weight superpositions of the $|a_i\rangle$ associated with the greatest and least eigenvalues, e.g., $(|a_{\min}\rangle + |a_{\max}\rangle)/\sqrt{2}$ [7–9]. The optimal measurement observables depend on A, too. Without information about A, therefore, conventional metrological phase estimation fails.

If H or A is unknown, one can first learn about it through quantum-process tomography [12–15]. However, process tomography requires many applications of e^{iH} or U_α, plus many measurements. The number of applications of a unitary quantifies resource usage in quantum computing and metrology. Hence tomography is costly. Furthermore, one often cannot leverage process tomography. For example, consider a magnetic field whose direction changes. We might wish to measure the field strength α at some instant. The probes must be prepared optimally beforehand.

Recently, [16] outlined a phase-estimation protocol for when information about A becomes available *after* the unitary operates. The protocol harnesses the mathematical equivalence between certain entanglement-manipulation experiments and closed timelike curves, hypothetical worldlines that travel backward in time [17–22]. In the protocol of [16], one entangles a probe and ancilla. After information about A becomes available, one effectively updates the probe's initial state, by measuring the ancilla, using the equivalence. This prescription inspires metrological protocols that leverage entanglement to circumvent requirements of prior information. Optics experiments have explored the relationship between entanglement manipulation and closed timelike curves [23,24]. Additionally, delayed-choice quantum-erasure experiments [25,26] resemble the protocol in [16] conceptually. However, metrological protocols inspired by closed timelike curves have not been reported.

We show that entanglement manipulation can enable optimal estimation of α, even sans information about A. We consider a common scenario: an arbitrary unbiased estimator $\hat{\alpha}$ is calculated from N measurement outcomes. The Fisher information (FI) I_α quantifies the outcome probabilities' sensitivity to small changes in α. I_α, defined below, limits the estimator's variance through the Cramér-Rao bound: $\mathrm{var}(\hat{\alpha}) \geq 1/(N I_\alpha)$. We theoretically prove that entanglement can boost the FI of α by 50%. Our protocol is optimal, achieving the FI of the optimal protocol that leverages knowledge of A. Using superconducting qubits, we demonstrate the advantage experimentally.

The next sections present and experimentally demonstrate four strategies for inferring about α without knowledge of the rotation axis $\hat{n}$. A single-qubit sensor can extract no information about α. Two time-travel-inspired protocols follow: *hindsight sensing* consumes a maximally entangled two-qubit state. The protocol achieves an FI of 1 if information about $\hat{n}$ becomes available eventually. *Agnostic sensing* requires a maximally entangled two-qubit state and an entangling measurement. The protocol achieves an FI of 1 even if $\hat{n}$ remains unknown. We compare these entanglement-boosted protocols to *entanglement-free sensing with an ancilla* whose FI is 2/3.

Single-qubit quantum sensor.—The simplest quantum sensor is a qubit probe subject to an unknown rotation, represented by $U_\alpha = \exp\left(-i\alpha\hat{n} \cdot \boldsymbol{\sigma}/2\right)$. The unknown rotation angle is α, $\hat{n} = \sin\theta\cos\phi\hat{x} + \sin\theta\sin\phi\hat{y} + \cos\theta\hat{z}$ defines the unknown rotation axis, and $\boldsymbol{\sigma} = (X, Y, Z)$ denotes a vector of Pauli operators. θ and ϕ denote the polar and azimuthal angles. Figure 1(a) illustrates the protocol: the probe is prepared in $|\psi\rangle$, evolves to $|\psi_\alpha\rangle := U_\alpha|\psi\rangle$, and is measured projectively. One aims to infer the rotation angle α.

Consider measuring the probe in an arbitrary basis $\{|i\rangle\}$. Outcome i occurs with probability $P_i = |\langle i|\psi_\alpha\rangle|^2$. The FI quantifies these probabilities' α sensitivity: $I_\alpha = \sum_{i=0,1}[(\partial_\alpha P_i)^2/P_i]$. The FI is upper bounded by the quantum Fisher information (QFI), $\mathcal{I}_\alpha$ [7,27]:

$$I_\alpha \leq \mathcal{I}_\alpha = 4(\langle\partial_\alpha\psi_\alpha|\partial_\alpha\psi_\alpha\rangle - |\langle\psi_\alpha|\partial_\alpha\psi_\alpha\rangle|^2). \quad (1)$$

The QFI, itself, is upper bounded by the maximum variance of the generator $\hat{n} \cdot \hat{\boldsymbol{\sigma}}/2$ of U_α: $\mathcal{I}_\alpha \leq 4\max_{|\psi\rangle}\{\mathrm{var}(\hat{n} \cdot \hat{\boldsymbol{\sigma}}/2)\} = 1$. Consider the many-trial limit (as $N \to \infty$). If $\hat{n}$ is known, all bounds (including the introduction's Cramér-Rao bound) can be saturated:

$$\mathrm{var}(\hat{\alpha}) = \frac{1}{NI_\alpha} = \frac{1}{N\mathcal{I}_\alpha} = \frac{1}{4N\max_{|\psi\rangle}\{\mathrm{var}(\frac{\hat{n}\cdot\hat{\sigma}}{2})\}} = \frac{1}{N}. \quad (2)$$

If $\hat{n}$ is unknown, neither saturation happens, typically [28].

Figure 1(b) depicts the protocol on the Bloch sphere. Without loss of generality, the rotation axis lies in the $\hat{x}$–$\hat{z}$ plane. We choose the pure initial state's Bloch vector
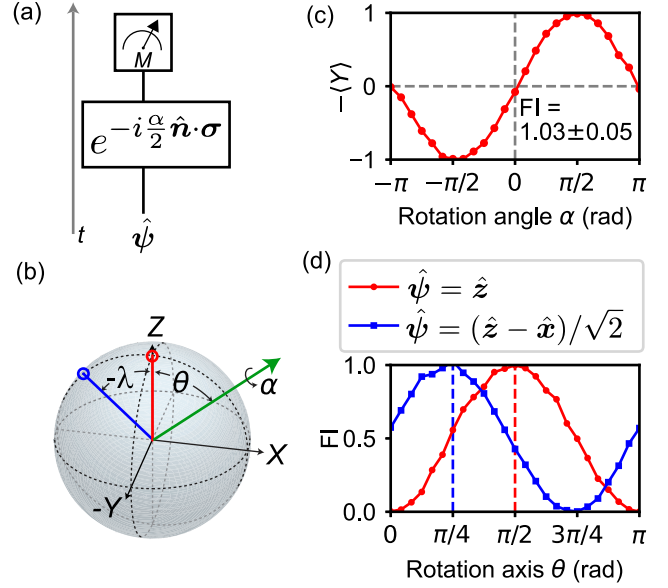

FIG. 1. Fisher information achievable with single-qubit sensor. (a) Protocol for sensing the rotation angle α. Time runs vertically, as in the closed-timelike-curve representation introduced later. (b) Bloch-sphere representation of the protocol. The red and blue lines represent possible initial states. The green arrow indicates the rotation axis. (c) Outcomes from preparing $\hat{\psi} = \hat{z}$, then rotating about the $\hat{x}$ axis through a varying rotation angle α. The red points and curve represent the measured $-\langle Y\rangle$ values, from which we infer the FI (± 1 standard deviation). (d) FI measured at various rotational axes parametrized by θ. If the initial state is $\hat{\psi} = \hat{z}$ (red curve), the FI fails to achieve its maximum value, except if $\theta = \pi/2$ specifies the rotation axis. An analogous statement concerns $\hat{\psi} = (\hat{z} - \hat{x})/\sqrt{2}$ (blue curve) and $\theta = \pi/4$.

to be $\hat{\psi} = \sin(\lambda)\hat{x} + \cos(\lambda)\hat{z}$, illustrating diverse metrological outcomes, from worst to optimal. Figure 1(b) shows two possible initial states, with $\lambda = 0$ (red) and $\lambda = -\pi/4$ (blue). The Supplemental Material [28] details single-qubit rotations' implementation. The rotation evolves the probe state to $|\psi_\alpha\rangle$. Our later analysis governs all $\alpha \in [-\pi, \pi]$, but illustrating with infinitesimal rotations $d\alpha$ first is instructive. An infinitesimal rotation displaces the Bloch vector by an amount $d\psi = \hat{n} \times \hat{\psi}d\alpha = \sin(\lambda - \theta)\hat{y}d\alpha = \hat{y}d\langle Y\rangle$. Therefore, an optimal final measurement is of Y.

Figure 1(c) displays data from optimal measurements. We show $-\langle Y\rangle$ at multiple α values for the initial state $\lambda = 0$ and rotation-axis parameter $\theta = \pi/2$. We calibrated and corrected for the $\approx 98\%$ measurement fidelity throughout this Letter [28]. Fitting the outcomes to a sinusoid, we infer the P_is at $\alpha = 0$. From them, we calculate $I_\alpha = 1.03 \pm 0.05$, consistently with the maximum predicted QFI.

Figure 1(d) displays the measured FI for various rotation axes. The red curve (initial state parametrized by $\lambda = 0$) shows that the maximum FI is achieved only when $\theta = \pi/2$. The blue curve (initial state with $\lambda = -\pi/4$)

shows a maximum FI only at $\theta = \pi/4$. These results illustrate an above-mentioned point: one can generally obtain the maximum FI about α only if prior knowledge about θ informs the probe's preparation and measurement. This limitation betrays a deeper problem with the single-qubit probe [28]: U_α has three unknown parameters, whereas a qubit has 2 degrees of freedom (d.o.f.). Estimating α, without knowing the rotation axis, is therefore typically impossible.

Hindsight sensing.—We relax the requirement of prior knowledge about $\hat{n}$, harnessing the connection between closed timelike curves and entanglement [21,22,56,57]. Consider preparing a maximally entangled (Bell) state [the ∪ symbol in Fig. 2(a)] between *two* qubits at time T_1. One can view this preparation as the chronology-violating trajectory of *one* qubit that travels backward in time, turns around at T_1, and continues forward in time [19–22]. We harness this connection to effectively choose a probe's initial state *in hindsight*.

Figure 2(a) illustrates this strategy. At T_1, we initialize a probe qubit and an ancilla qubit in a singlet. A unitary U_α rotates the probe's state about an unknown axis $\hat{n}$. Afterward, $\hat{n}$ is revealed; Eq. (2) can be satisfied. We measure the ancilla along an axis orthogonal to $\hat{n}$. The measurement projects the ancilla onto an optimal rotation-sensing state. The probe's state becomes orthogonal to the ancilla's. One can imagine that the time-traveling qubit in Fig. 2(a) is flipped at T_1. Hence closed timelike curves inspire our experiment.

In previous metrology protocols [58–61], an ancilla measurement determined whether the probe would undergo a final, information-acquiring measurement. Our protocol always features probe and ancilla measurements. The ancilla-measurement outcomes help us postprocess the data from probe-measurement outcomes to infer about α.

All four Bell states [11] serve equally well, we prove in [28]. We illustrate with the singlet, whose effectiveness we understand intuitively through the state's rotational invariance:

$$|\Psi^-\rangle = \frac{1}{\sqrt{2}}(|b\rangle_P|\bar{b}\rangle_A - |\bar{b}\rangle_P|b\rangle_A). \qquad (3)$$

P denotes the probe; and A, the ancilla. The structure of $|\Psi^-\rangle$ does not depend on the single-qubit basis $\{|b\rangle, |\bar{b}\rangle\}$; $|\Psi^-\rangle$ remains invariant under identical rotations of P and A. Denote by $|a_0\rangle$ and $|a_1\rangle$ the $-\hat{n} \cdot \hat{\sigma}/2$ eigenstates associated with the eigenvalues $+\frac{1}{2}$ and $-\frac{1}{2}$. Define the superpositions $|a^\pm\rangle \equiv (|a_0\rangle \pm |a_1\rangle)/\sqrt{2}$. Measuring the ancilla's $\{|a^\pm\rangle\}$ projects the probe onto an optimal state for measuring α.

Figure 2 details this protocol's experimental implementation. Using a parametric entangling gate, we prepare the probe and ancilla in a singlet [28]. We then rotate the probe and perform tomography on the probe-ancilla state. Figure 2(b) displays the measured probe expectation values
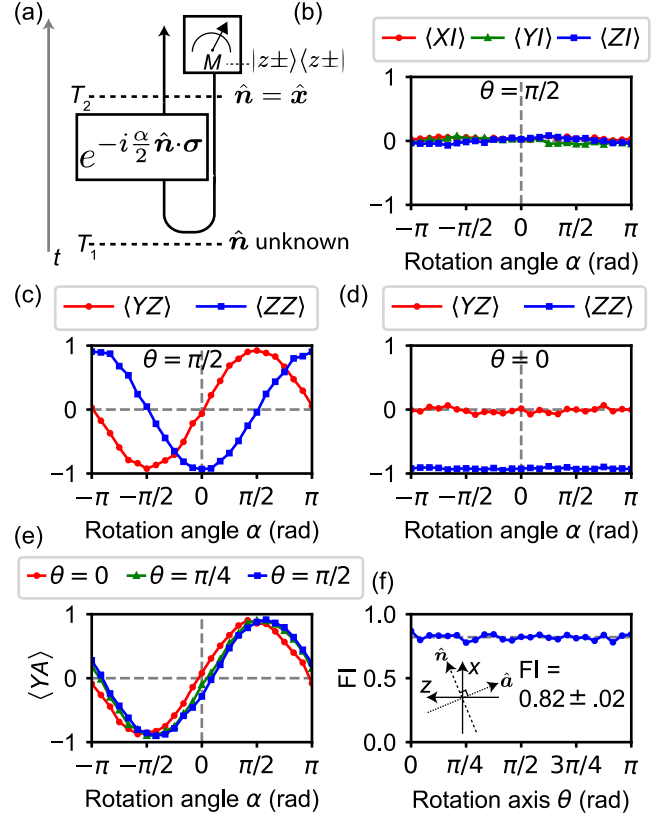

FIG. 2. Hindsight sensing. (a) Protocol for sensing the rotation angle α by mimicking a closed timelike curve. The ancilla's state effectively travels backward in time. It flips at T_1, becoming an optimal probe state. (b) No probe observable's expectation value carries information about α. (c) If the rotation is about the x axis (if $\theta = \pi/2$), the probe-ancilla correlators $\langle YZ \rangle$ and $\langle ZZ \rangle$ encode information about α. (d) For different rotations about the z axis ($\theta = 0$), the same correlators contain no information about α. (e) The correlator $\langle YA \rangle$ depends on the optimal ancilla observable to measure. $\langle YA \rangle$ is sensitive to the rotational angle α, at rotation axes parametrized by $\theta = 0$, $\pi/4$, and $\pi/2$. (f) From the correlator, we calculate the FI, for various rotational axes. The FI remains close to the optimal value, 1. The subfigure indicates the optimal ancilla measurement axis $\hat{a}$.

when $\theta = \pi/2$ parametrizes the rotation axis. These expectation values encode no information about α, the flat curves indicate. This lack is expected, since each qubit's reduced state is maximally mixed.

To learn about α, we calculate two-qubit correlators. Figure 2(c) illustrates with $\langle YZ \rangle$. Using entanglement, we reproduce the results of Fig. 1(c): measuring the ancilla's Z projects the probe's Bloch vector onto $\pm\hat{z}$, which are optimal for sensing α. However, the sensor's sensitivity depends on the rotation axis. $\langle YZ \rangle$ and $\langle ZZ \rangle$ cannot register rotations about the $\hat{z}$ axis ($\theta = 0$), Fig. 2(d) shows.

We interpret these results using closed-timelike-curve language [62]. When the qubits are initialized in a singlet at T_1, the probe is configured agnostically: for every axis $\hat{m}$, $\langle \sigma \cdot \hat{m} \rangle = 0$. The probe is waiting for the optimal-state

input from the future. The probe is rotated—and the ancilla's optimal basis, $\{|a^\pm\rangle\}$, is measured at T_2. The measurement projects the ancilla's state onto $|a^\pm\rangle$. This state is effectively sent backward in time and flipped into $|a^\mp\rangle$, to serve as the probe's time-T_1 state. Thus, the probe is retroactively prepared in the optimal state; is rotated with U_α; and, at T_2, undergoes a Y measurement.

Figure 2(e) demonstrates that we can obtain the maximum FI by measuring the ancilla $\hat{n}$-dependently, as by measuring $\{|a^\pm\rangle\}$. Figure 2(f) displays the FI obtained when $\theta \in [0, \pi]$ parametrizes the rotation axis. Regardless of the axis, we obtain a QFI of ≈ 0.82. This value is less the maximum possible QFI, due to the entangled-state preparation's finite fidelity [28].

Agnostic sensing.—The previous section's protocol lets us effectively choose the probe's initial state after U_α. Yet an entangling measurement, beyond the entangled initial state, enables an optimal sensing strategy that requires neither prior nor later knowledge of the rotation axis: what we term an *agnostic sensor*. Similar protocols have been studied in different settings [22,63,64].

Figure 3(a) sketches the protocol. Again, we initialize the probe and ancilla in a singlet, $|\Psi^-\rangle$. The probe undergoes an unknown rotation U_α, which maps $|\Psi^-\rangle$ to

$$|\Psi_\alpha^-\rangle = \frac{1}{\sqrt{2}}(e^{+i\frac{\alpha}{2}}|a_0\rangle_P|a_1\rangle_A + e^{-i\frac{\alpha}{2}}|a_1\rangle_P|a_0\rangle_A). \quad (4)$$

Finally, we perform an entangling measurement of $\{\Pi_0 := |\Psi^-\rangle\langle\Psi^-|, \Pi_1 := \mathbb{1} - \Pi_0\}$. The possible outcomes' probabilities are

$$P_0 := |\langle\Psi_\alpha^-|\Pi_0|\Psi_\alpha^-\rangle|^2 = \cos^2(\alpha/2) \quad \text{and} \quad (5)$$

$$P_1 := |\langle\Psi_\alpha^-|\Pi_1|\Psi_\alpha^-\rangle|^2 = \sin^2(\alpha/2). \quad (6)$$

This strategy produces the maximum FI about α, regardless of the rotation axis [7]. More broadly, Eq. (2) holds.

We can understand this result through closed timelike curves. If $\alpha = 0$, then U_α does not perturb the initial state $|\Psi^-\rangle$, and $P_0 = 1$. The ancilla-probe pair maps onto a particle traversing a closed timelike curve infinitely many times [21,22]. If $\alpha \neq 0$, U_α imprints α on the state. This experiment has a probability $P_0 < 1$ of successfully simulating a closed timelike curve. Knowing this success probability enables us to estimate α.

Figure 3 details our experimental demonstration. We prepare the singlet via an $\sqrt{i\text{SWAP}}$ gate [28]. The probe then undergoes U_α. We measure $\{\Pi_0, \Pi_1\}$ by rotating the ancilla, performing another $\sqrt{i\text{SWAP}}$, (this process maps the singlet onto separable states), and measuring each qubit's Z eigenbasis. From many trials, we infer P_0.

We measure P_0 for rotations about the $\hat{x}$, $\hat{y}$, and $\hat{z}$ axes, for several α values [Figs. 3(b)–3(d)]. As expected, $P_0 \propto \cos^2(\alpha/2)$, independently of the rotation axis. We fit P_0
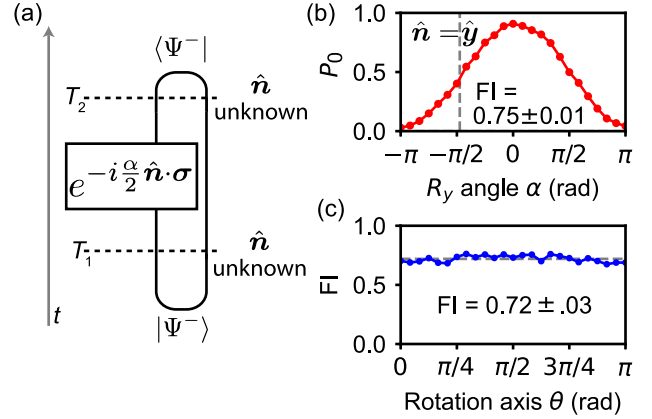

FIG. 3. Agnostic sensing. (a) Protocol: The probe and ancilla are prepared in a singlet. The probe is rotated, whereupon we measure whether the qubits remain in the singlet. (b) P_0 denotes the probability of obtaining a *yes*. From P_0, we infer the FI. Different plots follow from rotations about the $\hat{x}$, $\hat{y}$, and $\hat{z}$ axes. (c) FI inferred after various rotations in the $\hat{x}$–$\hat{z}$ plane.

near $\alpha = -\pi/2$ to infer the FI. Figure 3(e) displays the measured FI for rotation axes $\theta \in [0, \pi]$: regardless of the axis, $\mathcal{I}_\alpha = 0.72$.

The two-qubit gate's fidelity limits the FI, as in hindsight sensing. Agnostic sensing requires two such gates, so the infidelity impacts the FI more. This proportionality highlights a trade-off between quantum advantage and circuit depth.

Entanglement-free sensing with ancilla.—Let us compare the agnostic sensor with an optimal entanglement-free sensor. Imagine restricting the probes to identical single-qubit pure states. All pure states serve equally well, by symmetry: the rotation axis is unknown. Without loss of generality, therefore, we suppose the probes begin in $|\psi\rangle = |0\rangle$. Three independent, unknown parameters specify U_α: the rotation angle α, plus the rotation axis's zenith angle θ and azimuthal angle ϕ. One cannot estimate 3 parameters using a qubit, whose state encodes only 2 d.o.f. For every single-qubit probe, some (α, θ, ϕ) values yield $\mathcal{I}_\alpha = 0$. Hence, no single-qubit probes achieve Eq. (2), we prove in [28].

Nevertheless, one can estimate α without consuming entanglement, e.g., by performing quantum-process tomography on U_α [13,14]. Since $\hat{n}$ is unknown, the most reasonable prior distribution for $\hat{n}$ is uniform. We describe a strategy for garnering the greatest average FI inferable from any entanglement-free input: prepare the probe in a state $|\psi_j\rangle$, tagged with an ancilla state $|j\rangle$, with probability p_j:

$$\rho_0 = \sum_j p_j|\psi_j\rangle\langle\psi_j| \otimes |j\rangle\langle j|, \quad \text{wherein} \sum_j p_j = 1. \quad (7)$$

We show the following in [28]. First, for all ρ_0, the QFI about α, averaged over the $\hat{n}$, equals $2/3$. Second, not all ρ_0 achieve the first two equalities in Eq. (2). Third, we derive the form of

the states ρ_0 for which (i) $\mathcal{I}_\alpha = 2/3$ independently of $\hat{n}$ and (ii) the first two equalities in Eq. (2) hold. Examples include $\rho_\star = (|x+\rangle\langle x+| \otimes |1\rangle\langle 1| + |y+\rangle\langle y+| \otimes |2\rangle\langle 2| + |z+\rangle\langle z+| \otimes |3\rangle\langle 3|)/3$, where $|x+\rangle$ denotes the eigenvalue-1 X eigenstate, etc. Preparing and optimally measuring $\rho_\star$ yields a FI of $2/3$ about α [Eq. (C33) in [28]], irrespectively of $\hat{n}$. In [28] we describe our experimental implementation of this entanglement-free strategy, where we achieve an average axis-independent FI of 0.62, consistent with the theoretical maximum of $2/3$.

Discussion.—In [65], the authors distinguish a hierarchy of quantum sensors: some leverage energy-level quantization (type I), others leverage quantum coherence (type II), and others leverage entanglement (type III). We have introduced a type-III sensor. It achieves an advantage over the more-classical type-II sensors, when the resource is the number of times the unitary is applied. The 50% improvement in the QFI weighs against the cost of entanglement manipulation. One cost that we avoid is postselection: we discard no data. All measurement outcomes inform our inference of α, despite a known relationship between postselection and closed timelike curves [21,22].

Several opportunities suggest themselves. First, our protocol merits extending to optical [66] and solid-state systems that have concrete metrological applications. Second, our protocol may benefit phase estimation in quantum algorithms. Third, our experiment was inspired by the theoretical application of closed timelike curves to metrology [16]—specifically, to weak-value amplification, a technique for sensing interaction strengths [68–74]. One can experimentally implement the application to weak-value amplification or to a more general technique, partially postselected amplification [60]. Fourth, we anticipate our technique's usefulness in metrology subject to time constraints. For example, one may need to measure a time-varying field at some instant [75–77]. To date, optimal sensing strategies have required *a priori* knowledge about the unknown unitary's generator, A. Our agnostic protocol entails optimal state preparations and measurements without this knowledge.

[1] P. W. Shor, Algorithms for quantum computation: Discrete logarithms and factoring, in *Proceedings of the 35th FOCS* (IEEE, New York, 1994), pp. 124–134, 10.1109/SFCS.1994.365700.

[2] G. Brassard, P. Høyer, M. Mosca, and A. Tapp, Quantum amplitude amplification and estimation, Contemp. Math. **305**, 53 (2002).

[3] B. Bauer, S. Bravyi, M. Motta, and G. K.-L. Chan, Quantum algorithms for quantum chemistry and quantum materials science, Chem. Rev. **120**, 12685 (2020).

[4] Y. Suzuki, S. Uno, R. Raymond, T. Tanaka, T. Onodera, and N. Yamamoto, Amplitude estimation without phase estimation, Quantum Inf. Process. **19**, 75 (2020).

[5] S. Lloyd, S. Bosch, G. D. Palma, B. Kiani, Z.-W. Liu, M. Marvian, P. Rebentrost, and D. M. Arvidsson-Shukur, Quantum polar decomposition algorithm, arXiv:2006.00841.

[6] S. Lloyd, B. T. Kiani, D. R. M. Arvidsson-Shukur, S. Bosch, G. D. Palma, W. M. Kaminsky, Z.-W. Liu, and M. Marvian, Hamiltonian singular value transformation and inverse block encoding, arXiv:2104.01410.

[7] S. L. Braunstein and C. M. Caves, Statistical distance and the geometry of quantum states, Phys. Rev. Lett. **72**, 3439 (1994).

[8] V. Giovannetti, S. Lloyd, and L. Maccone, Quantum metrology, Phys. Rev. Lett. **96**, 010401 (2006).

[9] V. Giovannetti, S. Lloyd, and L. Maccone, Advances in quantum metrology, Nat. Photonics **5**, 222 (2011).

[10] A. Y. Kitaev, Quantum measurements and the Abelian Stabilizer Problem, Electron. Colloquium Comput. Complex. TR96 (1995), https://eccc.weizmann.ac.il/eccc-reports/1996/TR96-003/index.html.

[11] M. A. Nielsen and I. L. Chuang, *Quantum Computation and Quantum Information*, 10th Anniversary Edition (Cambridge University Press, New York, NY, 2011), 10.1017/CBO9780511976667.

[12] I. L. Chuang and M. A. Nielsen, Prescription for experimental determination of the dynamics of a quantum black box, J. Mod. Opt. **44**, 2455 (1997).

[13] G. M. D'Ariano and P. Lo Presti, Quantum tomography for measuring experimentally the matrix elements of an arbitrary quantum operation, Phys. Rev. Lett. **86**, 4195 (2001).

[14] J. B. Altepeter, D. Branning, E. Jeffrey, T. C. Wei, P. G. Kwiat, R. T. Thew, J. L. O'Brien, M. A. Nielsen, and A. G. White, Ancilla-assisted quantum process tomography, Phys. Rev. Lett. **90**, 193601 (2003).

[15] X. Song, M. Naghiloo, and K. Murch, Quantum process inference for a single-qubit Maxwell demon, Phys. Rev. A **104**, 022211 (2021).

[16] D. R. M. Arvidsson-Shukur, A. G. McConnell, and N. Yunger Halpern, Nonclassical advantage in metrology established via quantum simulations of hypothetical closed timelike curves, Phys. Rev. Lett. **131**, 150202 (2023).

[17] K. Gödel, An example of a new type of cosmological solutions of Einstein's field equations of gravitation, Rev. Mod. Phys. **21**, 447 (1949).

[18] M. S. Morris, K. S. Thorne, and U. Yurtsever, Wormholes, time machines, and the weak energy condition, Phys. Rev. Lett. **61**, 1446 (1988).

[19] C. H. Bennett, in *Proceedings of QUPON, Vienna, Austria* (2005), https://research.ibm.com/people/charles-bennett.

[20] G. Svetlichny, Time travel: Deutsch vs. teleportation, Int. J. Theor. Phys. **50**, 3903 (2011).

[21] S. Lloyd, L. Maccone, R. Garcia-Patron, V. Giovannetti, Y. Shikano, S. Pirandola, L. A. Rozema, A. Darabi, Y. Soudagar, L. K. Shalm *et al.*, Closed timelike curves via postselection: Theory and experimental test of consistency, Phys. Rev. Lett. **106**, 040403 (2011).

[22] S. Lloyd, L. Maccone, R. Garcia-Patron, V. Giovannetti, and Y. Shikano, Quantum mechanics of time travel through post-selected teleportation, Phys. Rev. D **84**, 025007 (2011).

[23] M. Ringbauer, M. A. Broome, C. R. Myers, A. G. White, and T. C. Ralph, Experimental simulation of closed timelike curves, Nat. Commun. **5**, 4145 (2014).

[24] C. Marletto, V. Vedral, S. Virzì, E. Rebufello, A. Avella, F. Piacentini, M. Gramegna, I. P. Degiovanni, and M. Genovese, Theoretical description and experimental simulation of quantum entanglement near open time-like curves via pseudo-density operators, Nat. Commun. **10**, 182 (2019).

[25] F. Kaiser, T. Coudreau, P. Milman, D. B. Ostrowsky, and S. Tanzilli, Entanglement-enabled delayed-choice experiment, Science **338**, 637 (2012).

[26] J.-C. Lee, H.-T. Lim, K.-H. Hong, Y.-C. Jeong, M. S. Kim, and Y.-H. Kim, Experimental demonstration of delayed-choice decoherence suppression, Nat. Commun. **5**, 4522 (2014).

[27] C. W. Helstrom, *Quantum Detection and Estimation Theory*, 1st ed. (Elsevier, New Year, 1976), Vol. 123, https://shop.elsevier.com/books/quantum-detection-and-estimation-theory/helstrom/978-0-12-340050-5.

[28] See Supplemental Material at http://link.aps.org/supplemental/10.1103/PhysRevLett.132.260801, which includes Refs. [7–9,11,29–55], for experimental details, data processing techniques, and further theoretical analysis of the sensing protocols.

[29] C. Gaikwad, D. Kowsari, C. Brame, X. Song, H. Zhang, M. Esposito, A. Ranadive, G. Cappelli, N. Roch, E. M. Levenson-Falk, and K. W. Murch, Entanglement assisted probe of the non-Markovian to Markovian transition in open quantum system dynamics, Phys. Rev. Lett. **132**, 200401 (2024).

[30] M. Boissonneault, J. M. Gambetta, and A. Blais, Dispersive regime of circuit QED: Photon-dependent qubit dephasing and relaxation rates, Phys. Rev. A **79**, 013819 (2009).

[31] T. Walter, P. Kurpiers, S. Gasparinetti, P. Magnard, A. Potočnik, Y. Salathé, M. Pechal, M. Mondal, M. Oppliger, C. Eichler, and A. Wallraff, Rapid high-fidelity single-shot dispersive readout of superconducting qubits, Phys. Rev. Appl. **7**, 054020 (2017).

[32] A. Ranadive, M. Esposito, L. Planat, E. Bonet, C. Naud, O. Buisson, W. Guichard, and N. Roch, Kerr reversal in Josephson meta-material and traveling wave parametric amplification, Nat. Commun. **13**, 1737 (2022).

[33] J. Rapin and O. Teytaud, Nevergrad—A gradient-free optimization platform, https://GitHub.com/FacebookResearch/Nevergrad (2018).

[34] F. Pedregosa, G. Varoquaux, A. Gramfort, V. Michel, B. Thirion, O. Grisel, M. Blondel, P. Prettenhofer, R. Weiss, V. Dubourg, J. Vanderplas, A. Passos, D. Cournapeau, M. Brucher, M. Perrot, and É. Duchesnay, Scikit-learn: Machine learning in Python, J. Mach. Learn. Res. **12**, 2825 (2011), http://jmlr.org/papers/v12/pedregosa11a.html.

[35] B. Nachman, M. Urbanek, W. A. de Jong, and C. W. Bauer, Unfolding quantum computer readout noise, npj Quantum Inf. **6**, 84 (2020).

[36] M. Werninghaus, D. J. Egger, F. Roy, S. Machnes, F. K. Wilhelm, and S. Filipp, Leakage reduction in fast superconducting qubit gates via optimal control, npj Quantum Inf. **7**, 14 (2021).

[37] S. Kundu, N. Gheeraert, S. Hazra, T. Roy, K. V. Salunkhe, M. P. Patankar, and R. Vijay, Multiplexed readout of four qubits in 3D circuit QED architecture using a broadband Josephson parametric amplifier, Appl. Phys. Lett. **114**, 172601 (2019).

[38] D. F. V. James, P. G. Kwiat, W. J. Munro, and A. G. White, Measurement of qubits, Phys. Rev. A **64**, 052312 (2001).

[39] M. G. A. Paris, Quantum estimation for quantum technology, Int. J. Quantum. Inform. **07**, 125 (2009).

[40] H. Cramér, *Mathematical Methods of Statistics* (Princeton University Press, Princeton, NJ, 1999), https://press.princeton.edu/books/paperback/9780691005478/mathematical-methods-of-statistics-pms-9-volume-9.

[41] C. R. Rao, Information and the accuracy attainable in the estimation of statistical parameters, in *Breakthroughs in Statistics: Foundations and Basic Theory*, edited by S. Kotz and N. L. Johnson (Springer, New York, NY, 1992), pp. 235–247, 10.1007/978-1-4612-0919-5_16.

[42] A. Fujiwara and H. Nagaoka, Quantum Fisher metric and estimation for pure state models, Phys. Lett. A **201**, 119 (1995).

[43] J. Liu, H. Yuan, X.-M. Lu, and X. Wang, Quantum Fisher information matrix and multiparameter estimation, J. Phys. A **53**, 023001 (2020).

[44] C. W. Helstrom, Quantum detection and estimation theory, J. Stat. Phys. **1**, 231 (1969).

[45] H. Zhu, Information complementarity: A new paradigm for decoding quantum incompatibility, Sci. Rep. **5**, 14317 (2015).

[46] T. Heinosaari, T. Miyadera, and M. Ziman, An invitation to quantum incompatibility, J. Phys. A **49**, 123001 (2016).

[47] S. Ragy, M. Jarzyna, and R. Demkowicz-Dobrzański, Compatibility in multiparameter quantum metrology, Phys. Rev. A **94**, 052108 (2016).

[48] F. Albarelli, M. Barbieri, M. G. Genoni, and I. Gianani, A perspective on multiparameter quantum metrology: From theoretical tools to applications in quantum imaging, Phys. Lett. A **384**, 126311 (2020).

[49] A. Z. Goldberg, L. L. Sánchez-Soto, and H. Ferretti, Intrinsic sensitivity limits for multiparameter quantum metrology, Phys. Rev. Lett. **127**, 110501 (2021).

[50] A. Fujiwara, Quantum channel identification problem, Phys. Rev. A **63**, 042304 (2001).

[51] S. Pang, J. Dressel, and T. A. Brun, Entanglement-assisted weak value amplification, Phys. Rev. Lett. **113**, 030401 (2014).

[52] S. Pang and T. A. Brun, Improving the precision of weak measurements by postselection measurement, Phys. Rev. Lett. **115**, 120401 (2015).

[53] S. Alipour and A. T. Rezakhani, Extended convexity of quantum Fisher information in quantum metrology, Phys. Rev. A **91**, 042104 (2015).

[54] W. Salmon, F. Salvati, C. K. Long, J. Smith, and D. R. M. Arvidsson-Shukur, Comment on: Extended convexity of quantum Fisher information in quantum metrology (to be published).

[55] J. Gallier, *Notes on the Schur complement* (2010), https://repository.upenn.edu/handle/20.500.14332/6664.

[56] T. A. Brun and M. M. Wilde, Simulations of closed timelike curves, Found. Phys. **47**, 375 (2017).

[57] J.-M. A. Allen, Treating time travel quantum mechanically, Phys. Rev. A **90**, 042107 (2014).

[58] D. R. M. Arvidsson-Shukur, N. Yunger Halpern, H. V. Lepage, A. A. Lasek, C. H. W. Barnes, and S. Lloyd, Quantum advantage in postselected metrology, Nat. Commun. **11**, 3775 (2020).

[59] J. H. Jenne and D. R. M. Arvidsson-Shukur, Unbounded and lossless compression of multiparameter quantum information, Phys. Rev. A **106**, 042404 (2022).

[60] N. Lupu-Gladstein, Y. B. Yilmaz, D. R. M. Arvidsson-Shukur, A. Brodutch, A. O. T. Pang, A. M. Steinberg, and N. Yunger Halpern, Negative quasiprobabilities enhance phase estimation in quantum-optics experiment, Phys. Rev. Lett. **128**, 220504 (2022).

[61] F. Salvati, W. Salmon, C. H. W. Barnes, and D. R. M. Arvidsson-Shukur, Compression of metrological quantum information in the presence of noise, arXiv:2307.08648.

[62] We do not precisely simulate a (postselected) closed timelike curve [21]: we discard no information through postselection. However, such curves motivate and provide intuition about our experiment [16].

[63] D. Girolami, A. M. Souza, V. Giovannetti, T. Tufarelli, J. G. Filgueiras, R. S. Sarthour, D. O. Soares-Pinto, I. S. Oliveira, and G. Adesso, Quantum discord determines the interferometric power of quantum states, Phys. Rev. Lett. **112**, 210401 (2014).

[64] H. Yuan, Sequential feedback scheme outperforms the parallel scheme for Hamiltonian parameter estimation, Phys. Rev. Lett. **117**, 160801 (2016).

[65] C. L. Degen, F. Reinhard, and P. Cappellaro, Quantum sensing, Rev. Mod. Phys. **89**, 035002 (2017).

[66] Full Bell-basis measurements are not feasible in optics. However, our agnostic-sensing protocol requires only a measurement of whether the probe-and-ancilla system is in a singlet. This measurement can be achieved with Hong-Ou-Mandel Interferometry [67].

[67] S. L. Braunstein and A. Mann, Measurement of the Bell operator and quantum teleportation, Phys. Rev. A **51**, R1727(R) (1995).

[68] J. Dressel, M. Malik, F. M. Miatto, A. N. Jordan, and R. W. Boyd, Colloquium: Understanding quantum weak values: Basics and applications, Rev. Mod. Phys. **86**, 307 (2014).

[69] J. Harris, R. W. Boyd, and J. S. Lundeen, Weak value amplification can outperform conventional measurement in the presence of detector saturation, Phys. Rev. Lett. **118**, 070802 (2017).

[70] S. Pang, J. Dressel, and T. A. Brun, Entanglement-assisted weak value amplification, Phys. Rev. Lett. **113**, 030401 (2014).

[71] L. Xu, Z. Liu, A. Datta, G. C. Knee, J. S. Lundeen, Y.-q. Lu, and L. Zhang, Approaching quantum-limited metrology with imperfect detectors by using weak-value amplification, Phys. Rev. Lett. **125**, 080501 (2020).

[72] Y. Aharonov, D. Z. Albert, and L. Vaidman, How the result of a measurement of a component of the spin of a spin-1/2 particle can turn out to be 100, Phys. Rev. Lett. **60**, 1351 (1988).

[73] I. M. Duck, P. M. Stevenson, and E. C. G. Sudarshan, The sense in which a "weak measurement" of a spin-1/2 particle's spin component yields a value 100, Phys. Rev. D **40**, 2112 (1989).

[74] O. Hosten and P. Kwiat, Observation of the spin hall effect of light via weak measurements, Science **319**, 787 (2008).

[75] W. Tang, F. Lyu, D. Wang, and H. Pan, A new design of a single-device 3d Hall sensor: Cross-shaped 3d Hall sensor, Sensors **18**, 1065 (2018).

[76] S. Wei, X. Liao, H. Zhang, J. Pang, and Y. Zhou, Recent progress of fluxgate magnetic sensors: Basic research and application, Sensors **21**, 1500 (2021).

[77] V. Stankevič, S. Keršulis, J. Dilys, V. Bleizgys, M. Viliūnas, V. Vertelis, A. Maneikis, V. Rudokas, V. Plaušinaitienė, and N. Žurauskienė, Measurement system for short-pulsed magnetic fields, Sensors **23**, 1435 (2023).